Proc. Natl. Acad. Sci. USA
Vol. 91, pp. 5070–5074, May 1994
Medical Sciences

Mice lacking α1(IX) collagen develop noninflammatory degenerative joint disease

(gene targeting/cartilage degeneration/osteoarthritis)

REINHARD FÄSSLER[†‡], PATRICK N. J. SCHNEGELSBERG[†§], JESSICA DAUSMAN[†], TAKASHI SHINYA[§], YASUTERU MURAGAKI[§], MARY T. MCCARTHY[§], BJORN R. OLSEN[§], AND RUDOLF JAENISCH[†¶]

[†]Whitehead Institute for Biomedical Research and Department of Biology, Massachusetts Institute of Technology, Nine Cambridge Center, Cambridge, MA 02142; and [§]Department of Cell Biology and Harvard Medical School, 260 Shattuck Street, Boston, MA 02115

Communicated by Darwin J. Prockop, January 14, 1994 (received for review September 20, 1993)

ABSTRACT **Type IX collagen is a nonfibrillar collagen composed of three gene products, α1(IX), α2(IX), and α3(IX). Type IX molecules are localized on the surface of type II-containing fibrils and consist of two arms, a long arm that is crosslinked to type II collagen and a short arm that projects into the perifibrillar space. In hyaline cartilage, the α1(IX) collagen transcript encodes a polypeptide with a large N-terminal globular domain (NC4), whereas in many other tissues an alternative transcript encodes an α1(IX) chain with a truncated NC4 domain. It has been proposed that type IX molecules are involved in the interaction of fibrils with each other or with other components of the extracellular matrix. To test this hypothesis, we have generated a mouse strain lacking both isoforms of the α1(IX) chain. Homozygous mutant mice are viable and show no detectable abnormalities at birth but develop a severe degenerative joint disease resembling human osteoarthritis.**

Type IX collagen is composed of three distinct gene products, α1(IX), α2(IX), and α3(IX) (for a review, see ref. 1). The three polypeptides are folded such that three triple-helical (COL) domains are separated and flanked by non-triple-helical (NC) domains. Type IX molecules are associated with type II-containing fibrils in cartilage and various other tissues, with the central and C-terminal COL domains forming a long arm along the fibrillar surface and the N-terminal COL domain projecting into the perifibrillar space as a short arm (2–4). In hyaline cartilage, the α1(IX) collagen gene is transcribed from an upstream promoter, generating a transcript that encodes a large N-terminal globular domain (NC4) (5), whereas in tissues such as vitreous humor (6, 7), chicken primary corneal stroma (8, 9), neural retina (10), and perinotochordal matrix (10–12), the use of an alternative downstream promoter and an alternative exon results in a shorter transcript encoding an α1(IX) chain with a 3-amino acid NC4 domain (13, 14).

The localization of type IX collagen to the surface of collagen fibrils and the orientation of the NC4 globular domain in the perifibrillar space in cartilage have led to the proposal that type IX molecules are involved in the interaction of fibrils with each other or with other components of the extracellular matrix (1). To test this hypothesis directly, we have used homologous recombination in embryonic stem (ES) cells to generate a mouse strain lacking both isoforms of the α1(IX) chain. Here we report that homozygous mutant mice are viable and show no detectable abnormalities at birth; with age, however, they develop a severe degenerative joint disease resembling human osteoarthritis (OA).

The publication costs of this article were defrayed in part by page charge payment. This article must therefore be hereby marked "*advertisement*" in accordance with 18 U.S.C. §1734 solely to indicate this fact.

MATERIALS AND METHODS

Targeting Vector. The phage YM911 carries a 14-kb fragment containing exons 6, 7, 8, and 1* of the *Col9a1* gene isolated from a DBA genomic library (14). The targeting vector pmCol9KOB extends from the 5′ end of the phage insert to the third *Hin*dIII site ≈1 kb downstream of exon 8 and thus contains part of the NC4 coding sequences (exons 6, 7, and 1*) and the first common exon to both the long and short forms of α1(IX) collagen (exon 8) (14). Two oligonucleotides containing an *Xho* I site were inserted into the unique *Sfi* I site present in exon 8. This *Xho* I site was used to insert the phosphoglycerate kinase–neomycin cassette (15) in the opposite transcriptional direction to that of the *Col9a1* gene. For counterselection, a phosphoglycerate kinase–thymidine kinase cassette (16) was cloned into the *Sal* I site of pmCol9KOB.

Electroporation of ES Cells and Generation of Chimeric Mice. D3 ES cells (17) were grown and electroporated as described (16, 18). In brief, the targeting vector was linearized at a unique *Kpn* I site, and 1×10^8 ES cells were electroporated with it and selected in G418 (GIBCO) alone or together with gancyclovir (Syntex, Palo Alto, CA). Individually picked colonies were screened by digesting genomic DNA with *Eco*RI or *Eco*RV and probing the Southern blots with a 450-bp *Hin*dIII–*Apa*LI fragment.

Chimeric mice from two independently targeted ES-cell clones mated with BALB/c or C57 mice transmitted the targeted *Col9a1* allele to their offspring. Chimeras with germ-line transmission were further bred with 129/sv females to establish an inbred line of mutant mice.

Northern Blot Analysis. Prior to genotyping, RNA from day 17.5 embryos was isolated by the LiCl/urea method (19). Approximately 20 μg of size-separated RNA was transferred to nylon membranes. After an overnight hybridization at 65°C in Denhardt's solution followed by two consecutive 30-min washes in 2× standard saline citrate (SSC)/0.1% SDS at room temperature and in 0.2× SSC/0.1% SDS at 65°C, the membrane was exposed to film for 3 days at −70°C. The predicted genotypes from the Northern blot analysis were confirmed by Southern blot analysis of DNA isolated from tails removed prior to the RNA isolation procedure. A 1.1-kb *Eco*RI fragment spanning the 3′ coding region of the *Col9a1* cDNA, the α-actin probe (16), and a 600-bp *Pst* I neomycin fragment (15) were labeled by random priming (20) using [^{32}P]CTP (Amersham).

Western Blot Analysis. Rib cages and vertebral columns of newborn pups were dissected and homogenized in 0.1 M Tris·HCl, pH 7.3/0.1 M sodium acetate. Samples were elec-

Abbreviations: ES, embryonic stem; mAb, monoclonal antibody; OA, osteoarthritis.

[‡]Present address: Department of Protein Chemistry, Max-Planck-Institut für Biochemie, D-8033 Martinsried bei München, Germany.
[¶]To whom reprint requests should be addressed.

trophoresed through SDS/PAGE gels and electroblotted onto nitrocellulose. The blots were blocked with 3% (wt/vol) skim milk (21) and treated with monoclonal antibody (mAb) against α1(II) collagen (mAb 2B1) (9) or α1(IX) collagen (mAb 23-5D1) (17). After washing, the blots were treated with goat anti-mouse IgG conjugated to alkaline phosphatase (Promega) and developed with the Bio-Rad alkaline phosphatase reagent kit.

Immunohistology and Histological Analysis. For embedding in paraffin, femurs fixed in 2.5% (vol/vol) gluteraldehyde in 0.1 M sodium cacodylate (pH 7.4) were decalcified for 1–2 weeks at room temperature in 10% EDTA in 0.1 M sodium cacodylate (pH 7.4). Sections were stained with hematoxylin/eosin or Weigert's iron hematoxylin, Fast green, and safranin-O. For immunofluorescence, cryostat sections of xiphoid process cartilage were digested with testicular hyaluronidase (80 units/ml, Sigma type I) for 30 min at 37°C and stained with polyclonal antibodies against the NC4 domain of α1(IX) collagen. The secondary antibody was fluorescein isothiocyanate-labeled goat anti-rabbit IgG (ImmunoSelect).

RESULTS

Generation of Mice with an Inactivated *Col9a1* Gene. The genomic organization of the 5′ portion of the *Col9a1* gene is illustrated in Fig. 1*A*. To generate mice lacking both the short and long forms of α1(IX), we disrupted exon 8 by inserting a phosphoglycerate kinase 1 (Pgk-1) promoter–neomycin gene cassette (15). This replacement vector provided 10 kb of homology at the 5′ end and 1.2 kb of homology at the 3′ end. To select against random integration, a viral thymidine kinase cassette (16) was included at the 3′ end of the vector. The linearized targeting vector was electroporated into the D3 ES-cell line (16–18). After double selection in G418 and gancyclovir, the enrichment of targeted clones was ≈15-fold. Targeted clones were identified by Southern blot analysis of genomic DNA digested with *Eco*RI or *Eco*RV (data not shown) and hybridized with probe HA (Fig. 1*A*). Of 350 doubly selected clones, 5 clones were identified as homologous recombinants. The average frequency of homologous recombination was ≈1 in 70 G418/gancyclovir-resistant

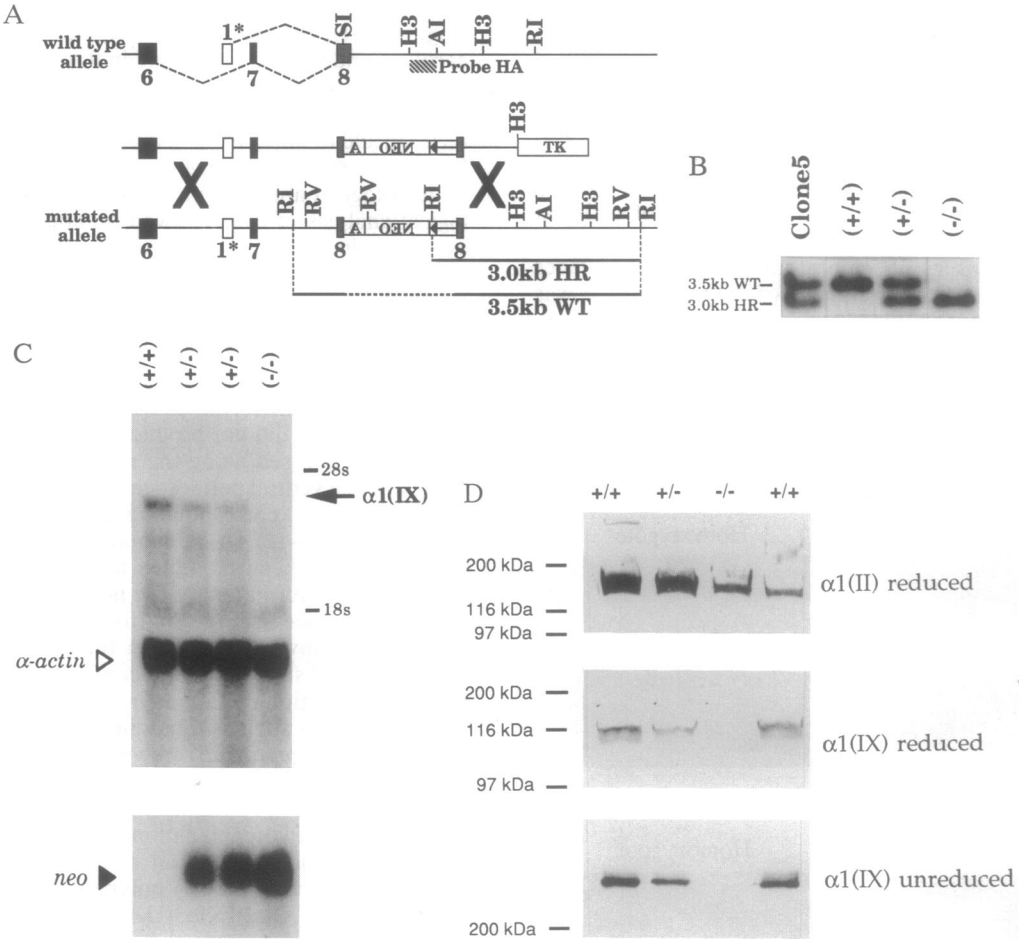

FIG. 1. Homologous recombination at the *Col9a1* locus. (*A*) Structure of the targeting vector pmCol9KOB with a partial restriction map of the *Col9a1* locus before (*Upper*) and after (*Lower*) homologous recombination. Initiation of transcription upstream of exon 1 (data not shown) and splicing of exons 6, 7, and 8 results in a long mRNA coding for the large NC4 domain. The mRNA coding for the small NC4 domain is generated by initiation of transcription between exons 6 and 1* followed by splicing of exon 1* to exon 8. The expected fragment sizes after *Eco*RI digestion of the wild-type (3.5 kb) and mutated (3.0 kb) *Col9a1* locus are shown (AI, *Apa*L I; H3, *Hin*dIII; RI, *Eco*RI; RV, *Eco*RV; SI, *Sfi* I). (*B*) Southern blot analysis. Genomic DNA from an injected cell line (clone 5) and from mouse tail DNA from progeny derived from a heterozygous intercross was digested with *Eco*RI or *Eco*RV (data not shown) and hybridized with a 3′ external probe, termed HA (see *A* hatched box labeled probe HA). The genotype at the *Col9a1* locus is indicated for each lane. The sizes of the DNA fragments are indicated in kilobases (kb). No additional rearrangements at the targeted locus were detected using a neomycin probe (data not shown). (*C*) Northern blot analysis of RNA from progeny of a heterozygous intercross. Total RNA from day 17.5 embryos was probed with a *Col9a1* cDNA fragment (arrow) located downstream of the neomycin insertion site, an α-actin cDNA (open arrowhead), and a neomycin cDNA fragment (solid arrowhead). The genotype at the *Col9a1* locus is indicated above each lane. (*D*) Western blot analysis of extracts from rib cage and vertebral column of newborn pups derived from a heterozygous intercross. Proteins were separated in 7.5% (*Top* and *Middle*) or 5% (*Bottom*) SDS/PAGE gels, electroblotted, and detected with mAbs against type II collagen (mAb 2B1) (*Top*) or α1(IX) collagen (mAb 23-5D1) (*Middle* and *Bottom*). The genotypes are indicated above each lane. The positions of globular molecular mass markers are indicated on the left.

clones, which implies an overall targeting efficiency of ≈1 in 1050 G418 clones.

Mice Homozygous for the Mutation Lack Col9a1 mRNA and Protein. Several chimeric mice derived from two targeted clones transmitted the mutant *Col9a1* gene to their offspring. Mice heterozygous for the mutation appeared normal and were intercrossed. Homozygous mutant offspring were identified by Southern blot analysis (Fig. 1*B*) and were normal in appearance. To investigate the effect of the mutation on Col9a1 gene expression, mRNA and protein levels were examined in wild-type, heterozygous, and homozygous mutant mice. Northern blot analysis of whole-embryo RNA showed reduced levels of *Col9a1* transcripts in heterozygotes and the complete absence of Col9a1 mRNA in homozygotes (Fig. 1*C*); this was confirmed by reverse transcription–PCR analysis (data not shown). The α1(IX) polypeptide (Fig. 1*D*) was not detected by Western blot analysis using an antibody reacting with the carboxyl region of the protein (22). The complete absence of the long form of α1(IX) collagen was confirmed by immunohistochemistry of sternal cartilage using an anti-NC4 antibody (Fig. 2).

Mutant Mice Develop a Degenerative Joint Disease. Mutant mice of different ages were analyzed for cartilage and bone abnormalities. No alterations were seen in young adults, but a progressive degenerative joint disease resembling human OA became apparent in homozygous mutant mice aged 4 months or older with the most prominent changes developing in the knee joints. These changes led to loss of articular cartilage; histology of 1-year-old animals showed total loss of cartilage in some areas of femoral and tibial joint surfaces (data not shown). At the periphery of the joints there was evidence of increased cartilage and bone formation with age. This led to shape changes in the joints. For example, in 9-month-old animals, examination of knee joints in the dissection microscope showed prominent shape changes of the articulating surfaces and surrounding bones in the absence of any inflammatory or immune response as judged by histological analysis. The upper part of the tibia had become wider than in the wild-type controls and the tibial cartilage surfaces were flattened, even concave, while the wild-type control animals showed convex tibial condyles (data not shown). The femoropatellar groove, while U-shaped in cross-section of control animals and in young (2 month old) mutants, was deep and V-shaped in 9-month-old homozygous mutant animals, with the underlying vascularization of the bone tissue shining through (Fig. 3*A*). Histological examination of the femoropatellar groove of knee joints of 9-month-old animals showed extensive alterations including the lack of cartilage in the center of the groove, the presence of chondrocytes with pyknotic nuclei, and reactive chondrocyte proliferation in the lateral parts of the groove, the latter leading to osteophyte formation (Fig. 3*C*). The subchondral bone was thinner in the mutant than in the normal cartilage. The femoral condylar surfaces were uneven in 9-month-old homozygous mutants and showed in some cases eroded areas filled with fibrous material (Fig. 3*B*). At this stage the articular surface of the patella also showed extensive alterations, such as fibrillation and a change in shape, from a smooth convex to a V-shaped form, congruent with the form of the femoropatellar groove (Fig. 3*D*). Histological analysis of femoral and tibial joint cartilage and subchondral bone in 9-month-old homozygous mutants showed surface irregularities, including fibrillation (Fig. 4*B*) and chondrocyte proliferation (Fig. 4*D*). Disorganization and thinning of subchondral bone was also apparent. In contrast to joint cartilage, other hyaline cartilages showed no histological abnormalities (data not shown). Also, histological analysis of eyes showed no apparent abnormalities, even in animals with extensive articular cartilage changes.

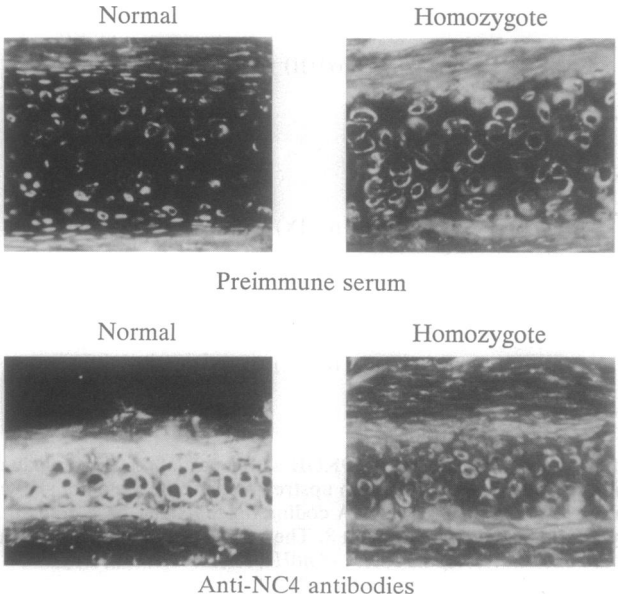

FIG. 2. Immunohistology of sternal xiphiod process cartilage from 3-month-old wild-type control and homozygous mutant mice. Photomicrographs showing reactivity of NC4 polyclonal antibodies with the cartilage matrix of normal wild-type mice (*Lower Left*) and lack of reactivity with the cartilage matrix from homozygous mutant mice (*Lower Right*). Preimmune serum did not react with tissue from either animal (*Upper*), but antibodies against α1(II) collagen showed intense staining of both types of cartilage (data not shown).

DISCUSSION

Gene targeting in ES cells was used to generate a mouse strain carrying a mutation in the first common exon encoding the long and short forms of α1(IX) collagen. Homozygous mutant embryos did not produce Col9a1 mRNA or protein. Col9a1 is expressed along the notochordal basement membrane and the ventral perinotochordal space where it is found between somites, corresponding to the anlagen of the vertebral arches (10–12). A null mutation of the gene might, therefore, have been predicted to cause defects during development and formation of the notochord. Contrary to this expectation, mice homozygous for the mutation were viable, exhibited no obvious defects in the vertebral column, and were of normal size. Several recently established mice bearing loss-of-function mutations in other widely and/or highly expressed genes such as tenascin (23), c-*src* (24), and nerve growth factor receptor (25) are viable and exhibit phenotypes that are much less severe than suggested by the expression patterns of the respective wild-type genes.

We consider two explanations for our observations. It is possible that the inactivation of the *Col9a1* gene and the resulting absence of α1(IX) polypeptides leads to the total absence of [α1(IX)α2(IX)α3(IX)] heterotrimers. If this were correct, it would suggest that type IX molecules are not essential for the assembly of extracellular matrices, including cartilage. Rather, type IX molecules might be important for the functional and structural integrity of specialized tissues, such as weight-bearing articular cartilage. Our results suggest that articular cartilage in the absence of type IX collagen is rendered more susceptible to damage resulting from mechanical stress. Alternatively, the α2(IX) and α3(IX) chains may form short-form type IX-like molecules in the absence of the α1(IX) chain. During development, such molecules may associate with type II fibrils and partially compensate for the lack of wild-type heterotrimeric type IX molecules. Proper functional and structural integrity of articular cartilage, however, would be impaired due to the absence of the α1(IX) chain (and thus the N-terminal globular domain NC4). As in

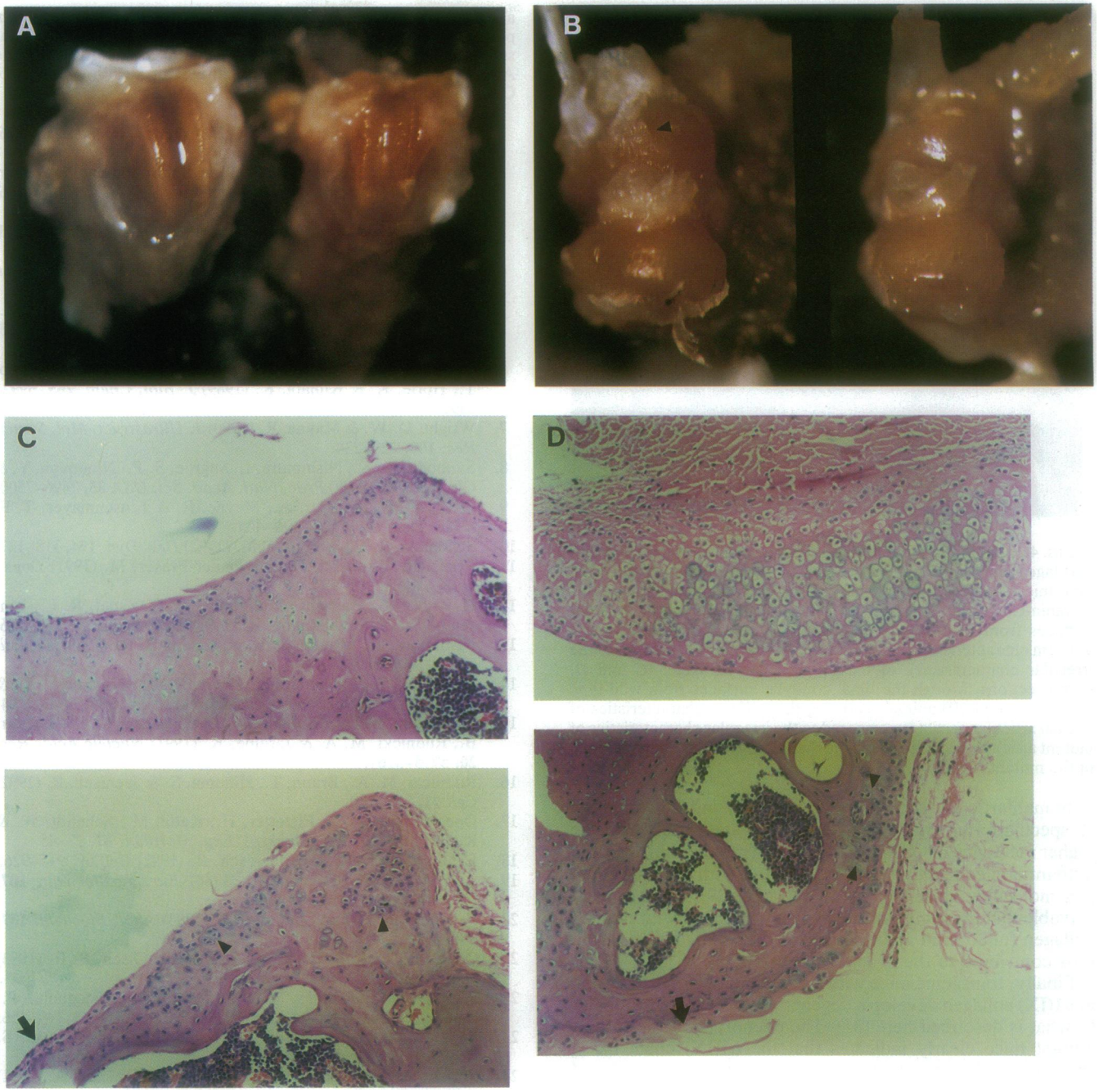

FIG. 3. Anatomy and histology of knee joint articular cartilage from 9-month-old wild-type control and homozygous mutant mice. (*A*) Photomicrograph (taken through the dissection microscope) showing the femoropatellar groove from wild-type (on the right) and homozygous mutant (on the left) animals. (*B*) Photomicrograph (taken through the dissection microscope) showing the femoral condyles from wild-type (on the right) and homozygous mutant (on the left) animals. Note the eroded area filled with fibrous material in the upper condyle in the mutant (arrowhead). This area was fused to the underlying meniscus, which had to be removed by sharp dissection to expose the articular surface. (*C*) Hematoxylin/eosin-stained cross-sections through the femoropatellar groove from wild-type (*Upper*) and homozygous mutant (*Lower*) mice. Note the even thickness and uniform staining of articular cartilage in the normal femoropatellar groove compared to the presence of fibrous tissue in the center (arrow) and signs of chondrocyte proliferation (arrowheads) toward the lateral margin of the femoropatellar groove in the mutant. (×100.) (*D*) Hematoxylin/eosin-stained section through the patella of wild-type (*Upper*) and homozygous mutant (*Lower*) animals. Compare the even articular surface of the normal patella with the uneven surface of the mutant patella that shows fibrillation (arrow) and areas of increased chondrocyte proliferation (arrowheads). The fibrous tissue to the right represents a portion of the ligamentum patella that folded over during embedding of the specimen. (×100.)

the first model, this would lead to the proposed decrease in mechanical strength. In either case, our data suggest that the α1(IX) chain plays an important role in maintaining the mechanical stability of articular cartilage and that its absence in mice leads to a degenerative joint disease with pathological changes comparable to some of those seen in human OA (26). While the changes observed in the mutant mice are by no means identical to those of human OA, several observations suggest a role for type IX collagen in joint diseases such as OA or rheumatoid arthritis. Patients suffering from OA have been reported to exhibit a decrease or absence of type IX collagen in articular cartilage (27), presumably due to an elevated stromelysin activity (28). Furthermore, it has been demonstrated that the amount of type IX collagen decreases

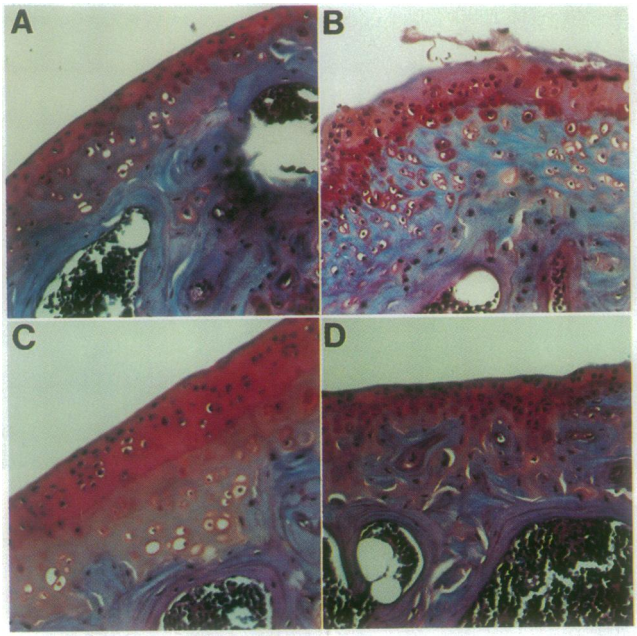

FIG. 4. Photomicrographs of sections through knee joint articular cartilage from 9-month-old wild-type control and homozygous mutant mice stained with Weigert's iron hematoxylin/Fast green/safranin-O. (*A* and *B*) Cross-sections through the femoral condylar surfaces from wild-type (*A*) and mutant (*B*) animals showing the uniform characteristics of normal articular cartilage compared to the irregular characteristics of mutant articular cartilage. (*C* and *D*) Cross-sections through the tibial condylar surfaces from wild-type (*C*) and mutant (*D*) animals showing the uniform characteristics of normal articular cartilage compared to the irregular characteristics of mutant articular cartilage; also note the sclerosis of subchondral bone in the mutant. (×50.)

in human articular cartilage with age (27), and it is tempting to speculate that this decrease may be associated with the higher incidence of OA in the elderly. In rheumatoid arthritis, autoantibodies reacting with type II and with type IX collagen molecules have been demonstrated (29, 30); it is conceivable that these autoantibodies may interfere with type IX collagen function in addition to that of type II collagen and thus contribute to the disease process.

Finally, transgenic mice with a dominant negative mutation in α1(IX) collagen develop a degenerative joint disease similar to what is described here (31). The phenotype of the *Col9a1* mutant mice clearly indicates that the α1(IX) chain has a specific function in articular cartilage that cannot be replaced by other molecules, as mice lacking a functional α1(IX) polypeptide develop a degenerative joint disease. Some characteristics of this disease, such as fibrillation, thinning of the cartilage, and chondrocyte proliferation, are similar to changes seen in human OA, but others, such as the changes observed in subchondral bone, are clearly different from the human disease. Nevertheless, the mutant mice described here should provide an excellent tool to gain insights into the functional role of type IX collagen in cartilage and serve as a model for rapid and premature noninflammatory joint destruction.

R.F. and P.N.J.S. have made equal contributions to this work. We thank Peter W. Laird and Gustavo Rosania for critically reading the manuscript and Ruth Curry for her expert technical assistance. R.F. was supported by a Max Kade fellowship. P.N.J.S. is a recipient of a Markey Biomedical Scientist Training Award. M.T.M. was supported by an Arthritis Foundation Fellowship. This research was supported by National Institutes of Health Grants AR36819 and AR36820 to B.R.O. and National Institutes of Health Grants R35-CA44339 and HL41434 to R.J.

1. Shaw, L. M. & Olsen, B. R. (1991) *Trends Biochem. Sci.* **16**, 191–194.
2. Vaughan, L., Mendler, M., Huber, S., Bruckner, P., Winterhalter, K. H., Irwin, M. I. & Mayne, R. (1988) *J. Cell Biol.* **106**, 991–997.
3. van der Rest, M. & Mayne, R. (1988) *J. Biol. Chem.* **263**, 1615–1618.
4. Wu, J.-J., Woods, P. E. & Eyre, D. R. (1992) *J. Biol. Chem.* **267**, 23007–23014.
5. Vasios, G., Nishimura, I., Konomi, H., van der Rest, M., Ninomiya, Y. & Olsen, B. R. (1988) *J. Biol. Chem.* **263**, 2324–2329.
6. Yada, T., Suzuki, S., Kobayashi, K., Kobayashi, M., Hoshino, T., Horie, K. & Kimata, K. (1989) *J. Biol. Chem.* **265**, 6992–6999.
7. Wright, D. W. & Mayne, R. (1990) *J. Ultrastruct. Mol. Struct. Res.* **100**, 224–234.
8. Svoboda, K. K., Nishimura, I., Sugrue, S. P., Ninomiya, Y. & Olsen, B. R. (1988) *Proc. Natl. Acad. Sci. USA* **85**, 7496–7500.
9. Fitch, J. M., Mentzer, A., Mayne, R. & Linsenmayer, T. F. (1988) *Dev. Biol.* **128**, 396–405.
10. Swiderski, R. E. & Solursh, M. (1992) *Dev. Dyn.* **194**, 118–127.
11. Perris, R., Krotoski, D. & Bronner-Fraser, M. (1991) *Development* **113**, 969–984.
12. Hayashi, M., Hayashi, K., Iyama, K., Trelstad, R. L., Linsenmayer, T. F. & Mayne, R. (1992) *Dev. Dyn.* **194**, 169–176.
13. Nishimura, I., Muragaki, Y. & Olsen, B. R. (1989) *J. Biol. Chem.* **264**, 20033–20044.
14. Muragaki, Y., Nishimura, I., Henney, A., Ninomiya, Y. & Olsen, B. R. (1990) *Proc. Natl. Acad. Sci. USA* **87**, 2400–2404.
15. McBurney, M. W., Sutherland, L. C., Adra, C. N., Leclair, B., Rudnicki, M. A. & Jardine, K. (1991) *Nucleic Acids Res.* **20**, 5755–5761.
16. Rudnicki, M. A., Braun, T., Hinuma, S. & Jaenisch, R. (1992) *Cell* **71**, 383–390.
17. Doetschman, T. C., Eistetter, H., Katiz, M., Schmidt, W. & Kemler, R. (1985) *J. Embryol. Exp. Morphol.* **87**, 27–45.
18. Li, E., Bestor, T. H. & Jaenisch, R. (1992) *Cell* **69**, 915–926.
19. Auffray, C. & Rougeon, F. (1980) *Eur. J. Biochem.* **107**, 303–314.
20. Feinberg, A. P. & Vogelstein, B. (1983) *Anal. Biochem.* **137**, 266–267.
21. Oh, S. P., Griffith, C. M., Hay, E. D. & Olsen, B. R. (1993) *Dev. Dyn.* **196**, 37–46.
22. Warman, M., Kimura, T., Muragaki, Y., Castagnola, P., Tamei, H., Iwata, K. & Olsen, B. R. (1993) *Matrix* **13**, 149–156.
23. Saga, Y., Yagi, T., Ikawa, Y., Sakakura, T. & Aizawa, S. (1992) *Genes Dev.* **6**, 1821–1831.
24. Soriano, P., Montgomery, C., Geske, R. & Bradley, A. (1991) *Cell* **64**, 693–702.
25. Lee, K.-F., Li, E., Huber, J., Landis, S. C., Sharpe, A. H., Chao, M. V. & Jaenisch, R. (1992) *Cell* **69**, 737–749.
26. Hamerman, D. (1989) *N. Engl. J. Med.* **320**, 1322–1330.
27. Brierley, V. H., Ayad, S. & Grant, M. E. (1991) *Biochem. Soc. Trans.* **19**, 379S.
28. Okada, Y., Shinmei, M., Tanaka, O., Naka, K., Kimura, A., Nakanishi, I., Bayliss, M. T., Iwata, K. & Nagase, H. (1992) *Lab. Invest.* **66**, 680–690.
29. Morgan, K., Clague, R. B., Collins, I., Ayad, S., Phinn, S. D. & Holt, P. J. L. (1987) *Ann. Rheum. Dis.* **46**, 902–907.
30. Boissier, M.-C., Chiocchia, G., Ronziere, M.-C., Herbage, D. & Fournier, C. (1990) *Arthritis Rheum.* **33**, 1–8.
31. Nakata, K., Ono, K., Myazaki, J.-I., Olsen, B. R., Muragaki, Y., Adachi, E., Yamamura, K.-I. & Kimura, T. (1993) *Proc. Natl. Acad. Sci. USA* **90**, 2870–2874.